Analyzing numerical grouted rockbolt behaviour in jointed pseudo-discontinuum models

Caitlin Fischer
Queen's Geomechanics and Geohazards Group, Department of Geological Sciences and Geological Engineering, Queen's University, Kingston, Ontario, Canada

Mark Diederichs
Queen's Geomechanics and Geohazards Group, Department of Geological Sciences and Geological Engineering, Queen's University, Kingston, Ontario, Canada

ABSTRACT: Pseudo-discontinuum numerical models, where discontinuities such as joints are represented discretely in an otherwise intact rockmass (termed "explicit" models in this paper), can demonstrate spatially variable rockmass response with movement along discrete geological structures. Explicit models used for the design of tendon rock support can therefore produce localized axial and shear loading in rockbolts crossing discrete joints. With strain-based and displacement-based failure criteria becoming increasingly common for predicting the performance of tendon ground support in underground excavations, the interaction between the rockmass and rockbolts must be understood. This paper demonstrates that the selected numerical rockbolt model and rockbolt input parameters govern the interaction between the rockmass and the rockbolt, and the displacements that occur in both systems.

Keywords: Explicit Numerical Modelling, Jointed Rock, Grouted Rockbolts, Rockbolt Models, Rockbolt Displacement, Strain-based Design.

1 INTRODUCTION AND BACKGROUND

Pseudo-discontinuum numerical rockmass models, where discontinuities such as joints are represented discretely in an otherwise intact rockmass (termed "explicit" models in this paper), show spatial variability in predicted rockmass displacements. Explicit models enable localized axial loads, shear loads, and combinations of the two to occur in modelled rockbolts crossing discrete joints. Strain-based and displacement-based design are becoming increasingly common for assessing the performance of rockbolts. Observational design for large-scale cavern projects, where access to support is lost as excavation proceeds, requires an understanding of the impact of movement along geological structures on permanent ground support. To predict realistic rockbolt displacements and strains for comparison to failure criteria, the interaction between the rockmass and the rockbolt must be understood. This research investigates the impact of the selected numerical bolt model on rockmass and bolt behaviour, and highlights methods for analyzing axial displacement in numerically modelled rockbolts. The sensitivity of bolt response to interface stiffness is also examined. Grouted rockbolts (resin-grouted rebar and cement-grouted rebar) are the focus of this research due to their

wide usage in civil engineering and mining engineering. Grouted rebar support is fully bonded to the rockmass using a grout material and generates shear resistance to movement through mechanical interlock between the bolt and the grout, and the grout and the rock. Resin-grouted rockbolts typically exhibit a stiffer bolt response, higher pull-out capacity, and lower axial strain limit compared to cement-grouted bolts. Both offer high tensile load resistance.

2 NUMERICAL MODELLING SCOPE AND INPUT PARAMETERS

Explicit rockmass models are developed using the 2D geotechnical Finite Element Method (FEM) software RS2 (Rocscience 2022). The represented rockmass has a Geological Strength Index (GSI) of 65 and is situated in an isotropic stress field at 1 km depth. A 10 m diameter tunnel (Figure 1) is excavated in five model stages: the first stage is unexcavated, the second stage is excavated with 100% induced stress load applied to the tunnel boundary, and the third, fourth, and fifth stages have 40%, 5%, and 0% induced stresses applied to the excavation boundary, respectively. 5 m long rockbolts are installed in 45-degree increments around the tunnel at the face (40% support pressure) and are loaded passively. Three bolts are labelled (B1-B3) for analysis in Section 3.

Fischer & Diederichs (2023) developed a detailed procedure for creating an explicit rockmass model for a given GSI. The GSI 65 rockmass in this paper uses the input parameters developed in Fischer & Diederichs (2023) and shown in Table 1.

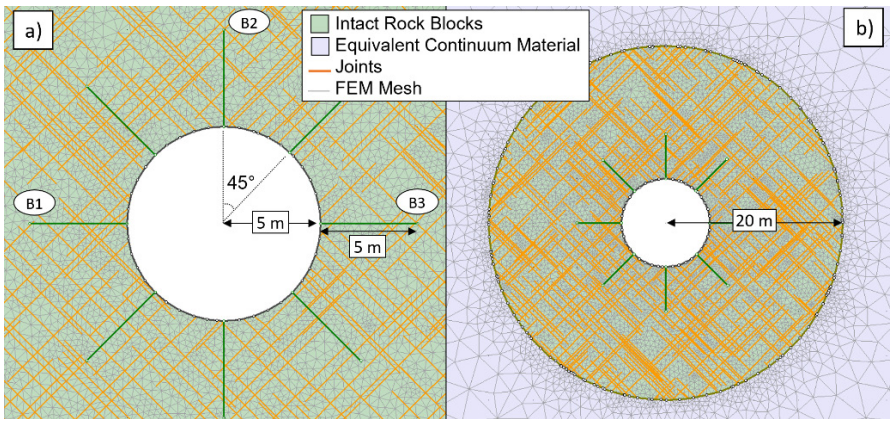

Figure 1. a) Excavated tunnel in the explicit GSI 65 rockmass with labelled rockbolts B1-B3. b) Explicit rockmass zone in the equivalent-continuum material that extends to pinned external boundaries.

Table 1. Explicit rockmass model input parameters (developed by Fischer & Diederichs 2023).

Intact Rock Block Input Properties		Baecher Joint Network Input Properties	
UCS (MPa)	120	Density (joints/m)	1.0
Intact Young's Modulus (GPa)	35.0	Number of Sets in Plane	2
Unit Weight (MN/m^3)	0.027	Inclinations (°)	45, -45
m_i	25	Trace Length (m)	8.1
Poisson's Ratio	0.25	JCS (MPa)	48.8
GSI*	85	JRC	12
*The application of GSI 85 to intact rock is used to decrease strength and stiffness to account for the additive effects of rock block scale and brittle spalling mechanisms (Diederichs 2007).		Base Friction Angle (°)	30.3
		Normal Stiffness, K_n (MPa/m)	90,000
		Shear Stiffness, K_s (MPa/m)	22,400

Two RS2 bolt models are used for modelling grouted rebar in this research (Table 2): the "Fully Bonded" bolt model (termed the "bonded model" in this paper) and the frictional "Swellex / Split Set" bolt model (termed the "sliding model" in this paper). While the mechanics of load transfer are complex and can be found in Rocscience (2023), the basic generation of axial force is a function of bolt extension as in Equation 1.

Table 2. Description of applicable support elements for modelling grouted rebar in RS2 (Rocscience 2023).

RS2 Fully Bonded Bolt Model	RS2 Frictional Swellex / Split Set Bolt Model
• Discretized at intersections with the FEM mesh. Each element acts independently, influencing the next through the rockmass. • Axial force in the bolt is determined from the elongation of the bolt element (eq. 1). • If axial force exceeds yield strength, bolt force is set to residual capacity. • The rock-grout and grout-bolt interfaces have infinite stiffness. The bolt is assumed to be fully bonded to the rock, even if the steel component of the bolt system has yielded.	• Discretized at intersections with the FEM mesh. Each segment directly impacts the next. • The strength and stiffness of the bolt/rock interface is considered. • If axial force exceeds bolt yield strength, axial force is set to residual. If bond shear strength is exceeded, bond force is set to residual. • Bolt elements are linked to the rockmass through springs with assigned "bond shear stiffness". Rocscience (2023) provides the detailed mathematical formulation.

$$F_{element} = \frac{AE}{L_{element}} \Delta u_{element} \quad (1)$$

Where F is the force in the bolt element, A is the bolt's cross-sectional area, E is the bolt modulus, L is the bolt element length, and Δu is the relative displacement between element nodes. For the bonded model, Δu is the same for the bolt element and the rock element to which it is attached. For the sliding model, a spring is added between the rock and the bolt. This "bond shear stiffness" is an important parameter controlling bolt response before the yield of either the interface (slip) or the bolt (rupture).

Where a rockbolt crosses a joint, axial forces are calculated in the bolt to resist movement for the section of bolt spanning the joint (assumed to be two bolt diameters in length). The bolt also resists joint movement through a dowel force (Dight 1982), which is a function of the joint displacement and is additive to the axial force generated by bolt strain. The section of bolt crossing the joint will fail if the dowel force exceeds the shear strength of the bolt (50% of tensile strength).

Input parameters for both bolt models are established from a review of literature on grouted rebar, with no distinctions made for differing grout materials (Table 3). Bolt tensile capacity, diameter, and modulus were specified for a standard rebar rock bolt. Bond strength was calculated from pull out test data (Kilic et al. 2002; Li et al. 2016; Bierman 2019), identifying a parametric range of 0.2 MN/m to 0.8 MN/m, depending on testing and materials. Bond stiffness was calculated using the relation presented by Holt (2017) for the interface shear stiffness of cement grout and limestone, which compared well to investigated ranges for bond shear stiffness used in numerical models of fully grouted rockbolts by Tomasone et al. (2020).

Table 3. Bolt input parameter summary.

Fully Bonded Bolt Model		Split Set Bolt Model	
Bolt Diameter (mm)	20.0	Tributary Area (mm^2)	314.2
Bolt Modulus (MPa)	200,000	Bolt Modulus (MPa)	200,000
Tensile Capacity (MN)	0.175	Tensile Capacity (MN)	0.175
Residual Tensile Capacity (MN)	0.0175	Residual Tensile Capacity (MN)	0.0175
		Bond Strength (MN/m)	0.35
		Residual Bond Strength (MN/m)	0.035
		Bond Shear Stiffness (MN/m/m)	25.13

3 NUMERICAL MODELLING RESULTS

Axial displacement data is presented in Figure 2 for both bolt models (bonded and sliding) and for two strength cases (realistic strength (Table 3) and infinite strength). Displacements presented are referenced to when support was installed. The sliding and bonded bolt models exhibit different

displacement and axial loading behaviour. Since the bonded model's displacement equals that of the rockmass, the large differential displacements across joints greatly affect load development in the bolt. Bonded bolts experience high axial forces at joint crossings (Figure 2b): the infinite strength bonded bolt shows elevated axial forces at each joint, and the realistic strength bonded bolt yields at the first three joints (where axial force drops to residual capacity in Figure 2b). The response of the sliding bolt model is less sensitive to the differential displacements across joints, since the sliding model considers interface shear stiffness, softening the impact of rockmass movements on the bolt (Figure 2a). Yield at joint crossings is not observed for the realistic strength sliding model. These results demonstrate that the bolt model selected can influence the occurrence of yield based on the displacement transfer mechanism from the rockmass to the bolt.

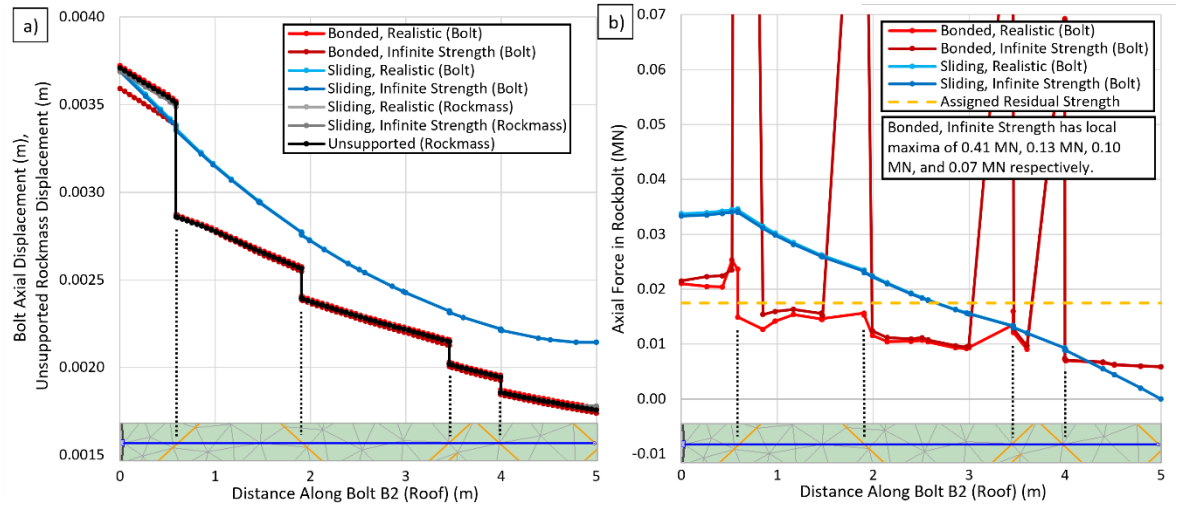

Figure 2. a) and b) Displacement and axial force data, respectively, for bolt B2. Dotted tie lines show bolt intersections with joints in the rockmass model image.

Figure 3 demonstrates the influence of bond interface shear stiffness on displacement results for the infinite strength, sliding bolt model. At low stiffnesses, little displacement is transferred to the rockbolt from the mobilizing rockmass, while at moderate stiffnesses (10-100 MN/m/m), a more realistic amount of rockmass displacement is transferred to the rockbolt.

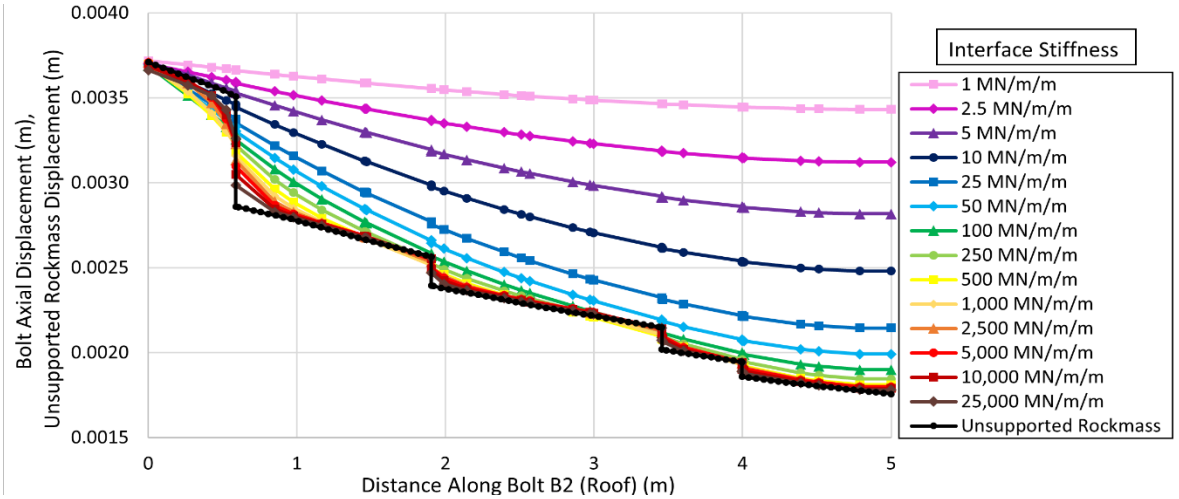

Figure 3. Displacement data for varying bond interface stiffnesses for the infinite strength, sliding bolt model (note: research literature indicates reasonable bond stiffnesses of 10 to 100 MN/m/m).

Figure 4 presents rockmass displacement data for bolts B1-B3. Bolt 1 exhibits the highest unsupported displacement at the excavation boundary, where a joint-bounded wedge is mobilizing

in the sidewall. Bolt 2 pins a partially bounded block in the roof, while Bolt 3 resists a mild slabbing-type failure in the right sidewall. Figures 4b-d display the change in rockmass displacement for each supported case compared to the unsupported case for each of B1-B3. Negative values denote a reduction in displacement with support. The results do not show a meaningful overall reduction of rockmass displacement with the installation of the bolts. Both increases and decreases in overall displacement are seen across Figures 4b-d, which can be attributed to the shuffling of rock blocks around the tunnel with the installation of support. Differential displacement across joint planes is reduced when rockbolts are installed, which is observed as local lows instantaneously changing to local highs in Figures 4b-d. Most bolts exhibit a holding effect on mobilizing material near the tunnel boundary (the 0 m position), shown by initial low difference values in Figures 4b-d.

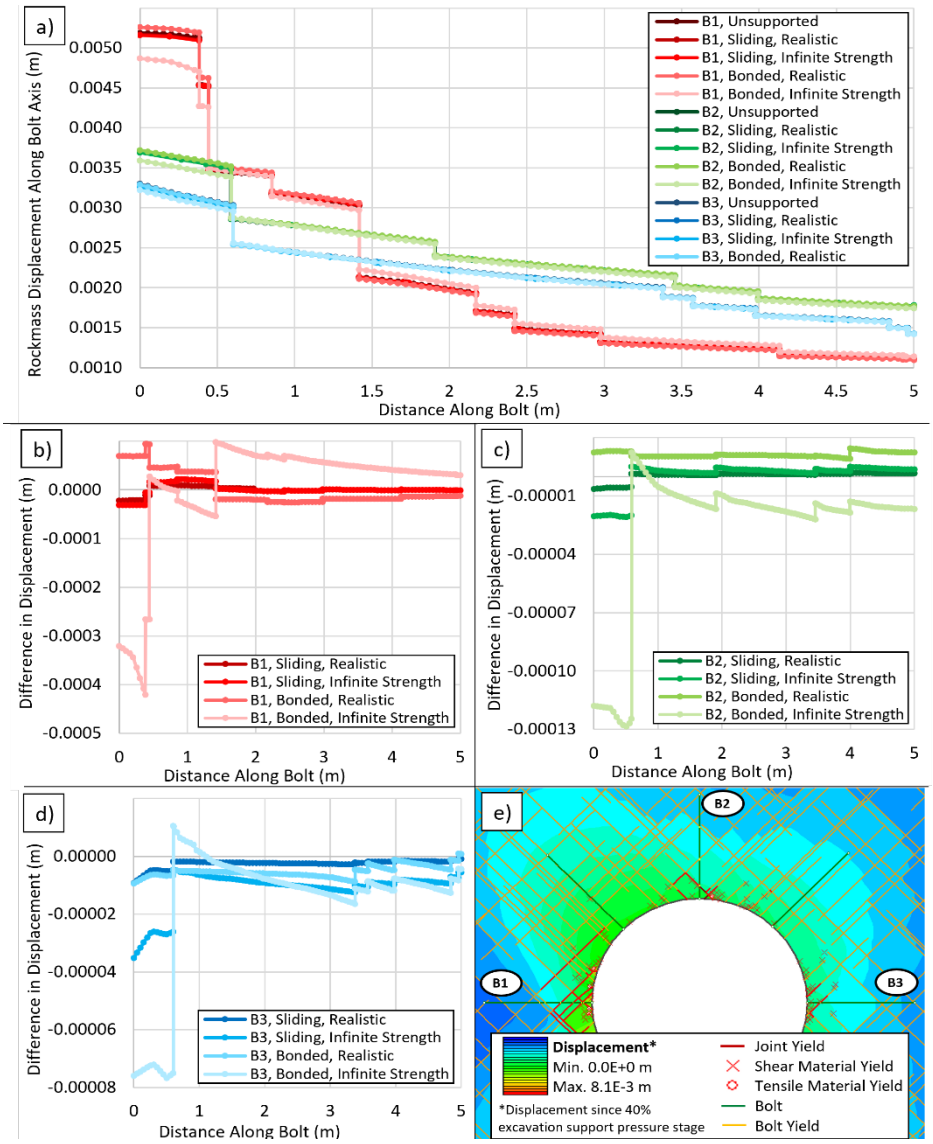

Figure 4. a) Rockmass displacement measured coaxially to rockbolts labelled in Figure 4e. b), c), and d) Difference between unsupported rockmass displacement and supported rockmass displacement for B1, B2, and B3, respectively. e) Rockmass displacement and yield for the bonded, realistic strength bolts.

4 CONCLUSIONS, LIMITATIONS, AND FUTURE WORK

The rockbolt model and input parameters selected govern the interaction between the rockmass and the rockbolt, and the displacements in both systems. The bonded bolt model investigated, which does

not consider bond interface properties, experiences displacement equal to that in the jointed rockmass and ruptures prematurely. The sliding bolt model investigated, which allows for some differential displacement between the rockbolt and rockmass, is more reflective of realistic grouted rockbolt behaviour. Shear interface stiffnesses of 10 – 100 MN/m/m result in reasonable displacement transfer to the rockbolt. Values closer to 10 MN/m/m better reflect a softer system (large bolt hole, cement grout), and values towards 100 MN/m/m better reflect a stiffer system (resin grout, small bolt hole). Bolt model nomenclature can pose a barrier to the selection of an appropriate bolt model, as the more representative model for grouted rebar in this study is named the "Swellex / Split Set" model.

The modelled rockbolts did not meaningfully decrease overall rockmass displacement for the explicitly modelled competent, mildly-moderately jointed rockmass. Without a discernable effect on convergence, ground support analysis becomes an assessment of what the rockmass does to the rockbolts, rather than what the rockbolts do to the rockmass. The increasing popularity of displacement- and strain-based support design requires an understanding of rockbolt displacement in both axial and shear directions. This research addresses only axial displacement, and future work should focus on shear displacement and strain. A meaningful incremental distance must also be selected with consideration for calculating strain (Graselli 2005; Forbes 2015). A limitation of the selected modelling method in this research is the absence of a dilational joint model (joints do not separate according to their roughness profile), limiting the ability to assess bolt impact on joint interlock. Bolt formulations in other geotechnical numerical modelling software that consider bond interface normal and shear properties should also be investigated in future work. Different rockmass qualities and stresses can also be investigated to assess the impact of modelled ground support on differing failure mechanisms and larger displacements.

ACKNOWLEDGEMENTS

The authors are grateful for research funding from the Natural Sciences and Engineering Research Council of Canada (NSERC) and the Nuclear Waste Management Organization (NWMO).

REFERENCES

Bierman, I.R., Gardner, L. & Piper, P. 2019. An evaluation of the bond strength of multiple resin bolt and capsule combinations through laboratory testing and applied methodologies. In: *Proc. of the Ninth International Conference on Deep and High Stress Mining*, Joughin, W. (ed), Johannesburg, pp. 175-190.

Diederichs, M.S. 2007. The 2003 Canadian Geotechnical Colloquium: Mechanistic interpretation and practical application of damage and spalling prediction criteria for deep tunnelling. *Canadian Geotechnical Journal* 44(9), pp. 1082–1116.

Dight, P.M. 1982. *Improvements to the stability of rock walls in open pit mines*. Ph.D. thesis. Monash University, Australia.

Fischer, C.P. & Diederichs, M.S. 2023. Elasto-Plastic and Post-Yield Weakening Jointed Rockmass Response in a Comparison of Equivalent-Continuum and Explicit Structural Models. *Canadian Geotech. J.* Accepted.

Forbes, B. 2015. *The Application of Distributed Optical Sensing for Monitoring Support in Underground Excavations.* Master's thesis. Queen's University, Canada.

Grasselli, G. 2005. 3D Behaviour of bolted rock joints: experimental and numerical study. *International Journal of Rock Mechanics and Mining Sciences* 42 (2005), pp. 13–24.

Holt, S.W. 2017. *Determination and Influence of Shear Strength Parameters of Material Interfaces Associated with Ground Support Systems.* Master's thesis. Royal Military College of Canada, Canada.

Kilic, A., Yasar, E. & Celik, A.G. 2002. Effect of grout properties on the pull-out load capacity of fully grouted rock bolt. *Tunnelling and Underground Space Technology* 17 (2002), pp. 355-362.

Li, C.C., Kristjansson, G. & Høien, A.H. 2016. Critical embedment length and bond strength of fully encapsulated rebar rockbolts. *Tunnelling and Underground Space Technology* 59 (2016), pp. 16–23.

Rocscience. 2022. RS2 2D Geotechnical Finite Element Analysis. Version 11.016. Rocscience: Toronto.

Rocscience. 2023. *Bolt Support Models.* Theory Manual. Rocscience: Toronto.

Tomasone, P., Bahrani, N. & Hadjigeorgiou, J. 2020. Practical considerations in the modelling of resin-grouted rockbolts. *Journal of the Southern African Institute of Mining and Metallurgy* 120 (6), pp. 385-392.